Article ID: 1006-8775(2024)01-0051-10

An Analysis of the Low Moving Speed of Landfalling Typhoon In-Fa in 2021

ZHENG Li-na (郑丽娜), LÜ Xin-gang (吕新刚), LI Rui (李　瑞)
(Jinan Meteorological Bureau of Shandong Province, Jinan 250102 China)

Abstract: The movement speed of Typhoon In-Fa (2021) was notably slow, at 10 km h^{-1} or less, for over 20 hours following its landfall in Zhejiang, China, in contrast to other typhoons that have made landfall. This study examines the factors contributing to the slow movement of Typhoon In-Fa, including the steering flow, diabatic heating, vertical wind shear (VWS), and surface synoptic situation, by comparing it with Typhoons Yagi (2018) and Rumbia (2018) which followed similar tracks. The findings reveal that the movement speed of Typhoons Yagi and Rumbia is most closely associated with their respective 500 hPa environmental winds, with a steering flow of 10–12 m s^{-1}. In contrast, Typhoon In-Fa's movement speed is most strongly correlated with the 850 hPa environmental wind field, with a steering flow speed of only 2 m s^{-1}. Furthermore, as Typhoon In-Fa moves northwest after landfall, its intensity is slightly greater than that of Typhoons Yagi and Rumbia, and the pressure gradient in front of Typhoon In-Fa is notably smaller, leading to its slow movement. Additionally, the precipitation distribution of Typhoon In-Fa differs from that of the other two typhoons, resulting in a weak asymmetry of wavenumber-1 diabatic heating, which indirectly affects its movement speed. Further analysis indicates that VWS can alter the typhoon's structure, weaken its intensity, and ultimately impact its movement.
Key words: landfalling typhoon; steering flow; diabatic heating; VWS
CLC number: P458.124 **Document code:** A
Citation: ZHENG Li-na, LÜ Xin-gang, LI Rui. An Analysis of the Low Moving Speed of Landfalling Typhoon In-Fa in 2021 [J]. Journal of Tropical Meteorology, 2024, 30(1): 51-60, https://doi.org/10.3724/j.1006-8775.2024.006

1 INTRODUCTION

The forecast and study of tropical cyclone movement have been essential topics in atmospheric sciences (Chen et al. [1]; Zhang et al. [2]; Fu et al. [3]). Tropical cyclones in the Northern Hemisphere tend to move northwestward (Chan and Williams [4]). However, the moving direction and speed of tropical cyclones are also affected by environmental factors such as steering flow (Wang et al. [5]; Chen et al. [6]), interaction with mid-latitude weather systems (Zhu et al. [7]; Yuan and Cao [8]; Fan et al. [9]) and topography (Bender et al. [10]; Chen et al. [11]). Typhoons after landfall can still bring rainstorms or even extreme rainstorms, resulting in severe disasters (Han et al. [12]; Huang et al. [13]; Wu et al. [14]). For example, Typhoon Nina in 1975, as a weakened tropical depression, moved inland and caused a devastating flood in Henan, China, claiming tens of thousands of lives (Li et al. [15]). Similarly, Super Typhoon Lekima (2019) caused heavy precipitation in Zhejiang, Jiangsu, and Shandong during its landfall and movement northward (Zheng et al. [16]). Given that typhoon tracks determine the distribution of heavy precipitation, numerous scholars have investigated the anomalous tracks of landing typhoons (Yang et al. [17]; Hill and Lackmann [18]). For instance, Zhang et al. [19] used numerical simulations to analyze the causes of the abnormal track of Typhoon Maggie (1999), attributing it to the influence of a neighboring tropical cyclone. Ma et al. [20] investigated the effect of dipole flow on typhoon tracks from the perspective of environmental fields. Duan et al. [21] discussed the causes of the abnormal tracks of Typhoons Aere (2011) and Meari (2011) based on energy dispersion. Additionally, several scholars studied the causes of anomalous typhoon tracks (Zheng et al. [22]; Zhang and Zheng [23]; Wang et al. [24]).

In general, due to the near-surface friction effect, the input kinetic energy of the lower-layer typhoon circulation rapidly reduces after typhoon landfall, and the inflow and pumping effect within typhoon circulation weakens (Yuan et al. [25]; Li and Pu [26]; Wang and Ying [27]). Meanwhile, since the water vapor on the underlying surface decreases after typhoon landfall, the warm-core structure of a typhoon is unable to be maintained, resulting in a rapid weakening of typhoon intensity (Huang and Chen [28]; Zhang et al. [29]). However, owing to the incursion of cold air (Zhao et al. [30]; Powell et al. [31]), the typhoon transition can appear after landfall under the interaction with mid-latitude circulation systems (Zhao [32]; Zeng et al. [33]) or favorable topography (Smith and Thomsen [34]; Yang et al. [35]), which can make the low-pressure circulation of the weakened typhoon to develop and strengthen again. According to Zhu et al. [36], the speed of a closed low pressure is inversely proportional to the strength of the system, so the strengthening or weakening

Received 2023-01-11; **Revised** 2023-11-15; **Accepted** 2024-02-15
Funding: Natural Science Foundation of Shandong Province (ZR2021MD012); CMA Special Fund for Innovation and Development (CXFZ2023J015)
Biography: ZHENG Li-na, Professor-level Senior Engineer, primarily undertaking research on extreme weather and tropical cyclones.
Corresponding author: ZHENG Li-na, e-mail: jnzln0103@163.com

of typhoons also affects the speed of typhoons to some extent.

Currently, there are numerous studies focusing on the intensity and movement tracks of typhoons, shedding light on the mechanisms behind variations in intensity and track. The track and intensity of a typhoon determine the distribution of typhoon-induced wind and precipitation and the degree of potential disasters. It is important to note that abnormally low or high typhoon movement speeds not only impact the prediction of typhoon-induced wind and precipitation but also influence the timing of typhoon defense measures. According to statistics, the moving speed of typhoons generated in the northwest Pacific Ocean is typically 20–30 km h^{-1} after landfall, and it can reach 40 km h^{-1} or more as typhoons weaken (Zhu et al. [36]). However, Typhoon In-Fa (2021), which formed in the northwest Pacific on July 18, made landfall in Zhejiang Province on July 25, weakened, and dissipated on July 30, with a lifespan of 12 days. Throughout this period, the typhoon maintained a slow speed of approximately 10 kilometers per hour. This sluggish movement resulted in severe flooding disasters in various parts of China, perplexing weather forecasters who questioned the unusually slow speed of the typhoon. The inaccurate assessment of Typhoon In-Fa's movement speed by forecasters led to deviations between forecasted and observed precipitation ranges and intensities, and missed opportunities to issue disaster warnings in certain areas. In order to study the cause of the low moving speed of Typhoon In-Fa, Typhoons Yagi (2018) and Rumbia (2018), which had similar tracks to that of Typhoon In-Fa, are used for comparative analysis. This study deepens the understanding of the physical mechanisms that influence typhoon moving speed.

The remainder of this paper is organized as follows. Section 2 briefly introduces the data and methods used in this study. Section 3 describes the movement characteristicsof Typhoon In-Fa. Section 4 reveals the causes of the low moving speed of Typhoon In-Fa, which include the influences of steering flow, diabatic heating, VWS, and surface situation. Finally, the main conclusions and discussion are shown in section 5.

2 DATA AND METHODS

2.1 *Data*

The datasets used in this study are the 1-hour typhoon information (center position, intensity, and moving speed) provided by the typhoon website of the National Meteorological Center, the 1-hour observed precipitation data provided by the China Meteorological Administration, and the reanalysis data provided by the National Centers for Environmental Prediction (NCEP). Among them, the elements of the reanalysis data include geopotential height, temperature, wind field, and latent and sensible heat fluxes at the sea (land)-air interface, with spatio-temporal resolutionsof 0.5° × 0.5° and 1 hour. The calculated diabatic heating is the sum of sensible and latent heat fluxes in this study. Note that the negative heat flux at the sea (land)-air interface indicates that the atmosphere provides heat to the ocean (land), i.e., the atmosphere heats the ocean (land). Conversely, the positive heat flux indicates that the ocean (land) heats the atmosphere.

2.2 *Methods*

2.2.1 PROCESSING OF TYPHOON TRACK DATA

Suppose the position of a typhoon at time t is $t_x(\mathrm{lon}_x, \mathrm{lat}_x)$ and the position at time $t+1$ is $t_{x+1}(\mathrm{lon}_{x+1}, \mathrm{lat}_{x+1})$. The distance between the two adjacent moments divided by the interval time is regarded as the moving velocity of the typhoon. Decompose this moving velocity on the X-axis and Y-axis. Since the unit longitude difference in the Northern Hemisphere decreases with increasing latitude, the u-component and v-component are expressed as Eqs. 1 and 2, respectively.

$$u = \frac{\cos(\mathrm{lat}_x)(\mathrm{lon}_{x+1} - \mathrm{lon}_x) * 111}{t_{x+1} - t_x} \tag{1}$$

$$v = \frac{(\mathrm{lat}_{x+1} - \mathrm{lat}_x) * 111}{t_{x+1} - t_x} \tag{2}$$

where the units of u-component and v-component are km h^{-1}, "lon" the longitudes, and "lat" the latitudes. The unit longitude (latitude) difference is approximately 111 km.

2.2.2 PROCESSING OF THE ENVIRONMENTAL WIND FIELD

In environmental wind fields, the typhoon circulations need to be removed, and the kinetic separation method is applied in this paper. The core idea of this method is that in the environmental field containing typhoon circulation, the vorticity field of a typhoon is typically one to two orders of magnitude larger than that of the external environmental field and has a relatively clear boundary. The wind field obtained by the vorticity inversion of a typhoon can be regarded as the wind field of the typhoon. The environmental wind field is obtained by subtracting the typhoon wind field data from the initial reanalysis wind field data.

With a typhoon center as the center of the circle, the values at the points on the circle with different latitude distances from the typhoon center are taken to form the environmental wind field. For example, draw circles with a radius of 5 latitudes from a typhoon center. In this way, we can obtain several circles from 1000 hPa to the tropopause. Then, points are taken on each circle. If the taken points are not on the grid, we use the three-dimensional bilinear interpolation method to obtain the values on the corresponding grid points. The data on these circles constitute the environmental wind field with a radius of 5 latitudes from the typhoon center.

2.2.3 CALCULATION OF ENVIRONMENTAL VWS

Referring to the method described in Wu and Wang [37], we calculate the average wind speed of the meridional and zonal wind fields at 200 hPa and 850 hPa in the 10° × 10° square grid area centered on the typhoon center. Then, we calculate the vector difference of the regional average wind velocities between the two layers (Eq. 3).

$$V_{\mathrm{vws}} = \sqrt{(u_{200} - u_{850})^2 + (v_{200} - v_{850})^2} \tag{3}$$

where V_{vws} represents the intensity of the environmental VWS, u_{850} and u_{200} indicate the average zonal wind speed at the 850 hPa and 200 hPa, respectively, and v_{850} and v_{200} denote the average meridional wind speed at the 850 hPa and 200 hPa, respectively. In this study, we use the classification criterion in Wingo and Cecil [38] to classify the V_{vws} into three grades: weak V_{vws} (<5 m s^{-1}), moderate V_{vws} (5–10 m s^{-1}) and strong V_{vws} (>10 m s^{-1}).

With the typhoon center as the original point, the *Y*-axis direction is 0° (or 360°). The direction of the VWS is represented by the angle between it and the *Y*-axis in the clockwise direction.

In this paper, the center position of the three typhoons (In-Fa, Yagi and Rumbia) provided by the National Meteorological Center during the study period is compared with those determined by the NCEP reanalysis data. The result shows that the center position deviation of the above two is within 0.3°. Therefore, using the typhoon location information provided by the National Meteorological Center, the typhoon vortex can be removed from the NCEP reanalysis data, and then the environmental wind field and vertical wind shear affecting the typhoon can be calculated.

3 MOVEMENT CHARACTERISTICS OF TYPHOON IN-FA

Typhoon In-Fa was generated in the northwest Pacific Ocean at 1800 (Coordinated Universal Time, UTC) on July 17, 2021, and then it moved northwestward. At 04:30 on July 25, this typhoon made landfall on the coast of Putuo District, Zhoushan City, Zhejiang Province, and continued to move northwestward after entering inland. Then, it turned northward in Anhui at 1200 UTC on July 28. At 1800 UTC on July 29, the typhoon entered the Bohai Sea and turned to move northeastward. At 0900 UTC on July 30, it weakened and transformed into an extratropical cyclone in the Bohai Sea. Two typhoons with similar tracks to Typhoon. In-Fa, namely Typhoons Yagi (2018) and Rumbia (2018), are selected for comparative analysis in this research. Typhoons Yagi and Rumbia were generated in the northwest Pacific Ocean with northwestward tracks, and they both made landfall on the coast of Zhejiang. In addition, Typhoons Yagi and Rumbia still moved northwestward after landfall. Typhoon Yagi turned northward in Anhui, and Typhoon Rumbia turned northward in Henan. For comparison, the periods when the intensity of the three typhoons were tropical storms (the near-surface maximum wind speed near the centers was 17.2–24.4 m s^{-1}) and the typhoons moved northwestward, and the underlying surface of the three typhoons was plain, i.e., comparative periods, are selected in this research (Fig. 1).

Figure 2 shows the moving speed of the three typhoons during the comparative periods. For Typhoon Yagi (2018), the initial speed in the comparative period was 39 km h^{-1}, and it decreased to 30 km h^{-1} after six hours and approximately 25 km h^{-1} after 16 hours. Typhoon Rumbia (2018) moved slightly slower than Typhoon Yagi (2018), with the initial speed being about 32 km h^{-1} in the comparative period. After 10 hours, the moving speed of Typhoon Rumbia decreased to 20 km h^{-1}. During the first two hours of the comparative period, the speed of Typhoon In-Fa (2021) was approximately 7 km h^{-1}, and then the speed increased slightly and remained at 10 km h^{-1}. The intensity of the three typhoons is comparable,

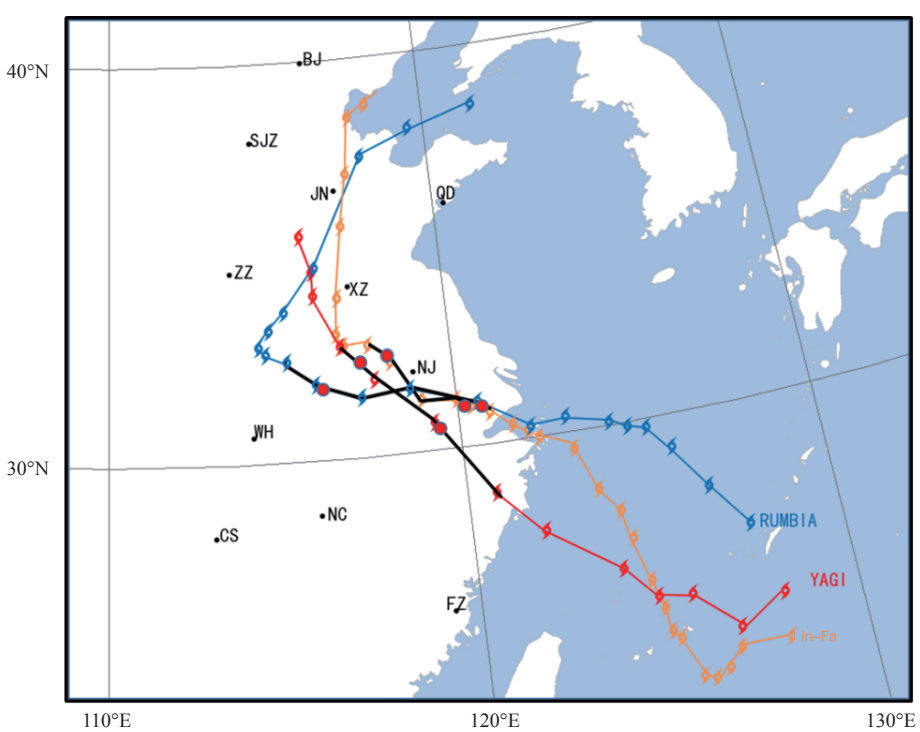

Figure 1. Tracks of Typhoons Yagi (2018), Rumbia (2018) and In-Fa (2021). The black curved lines represent the tropical storm phase, with the comparison period between the two red dots on the track.

and the underlying surfaces they traveled through are relatively similar. Under such situations, why did Typhoon In-Fa (2021) move overly slowly? In the following section, we will focus on the causes.

4 CAUSES OF THE LOW MOVING SPEED OF TYPHOON IN-FA (2021)

4.1 *Effect of the steering flow*

The role of the steering flow in the movement of typhoons cannot be ignored. Wu and Wang [37] pointed out that the movement of tropical cyclones is essentially influenced by the large-scale steering flow. Adem and Lezama's [39] numerical experiments showed that under the condition of constant Coriolis parameters, the positive pressure symmetric vortex will strictly move along the uniform basic flow, which can be considered as the large-scale environment flow is the steering flow. However, in the actual atmosphere, a tropical cyclone cannot be a strict axisymmetric vortex, so there is a certain deviation between the movement of a tropical cyclone and the steering flow (Chan and Gray [40]). Fig. 3 presents the correlations of the typhoon moving speed with the

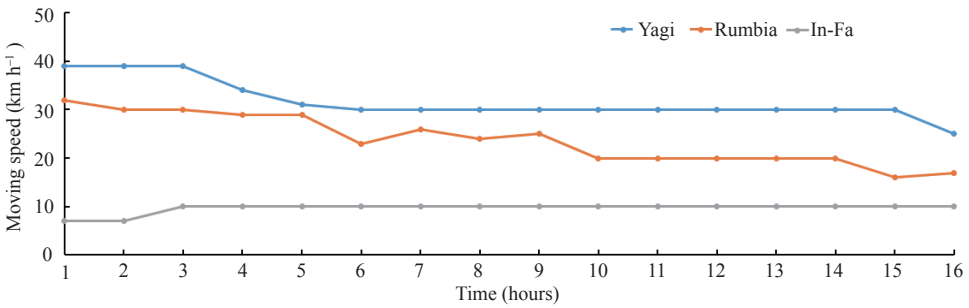

Figure 2. The corresponding speed of movement of Typhoons Yagi, Rumbia, and In-Fa in the comparison phase.

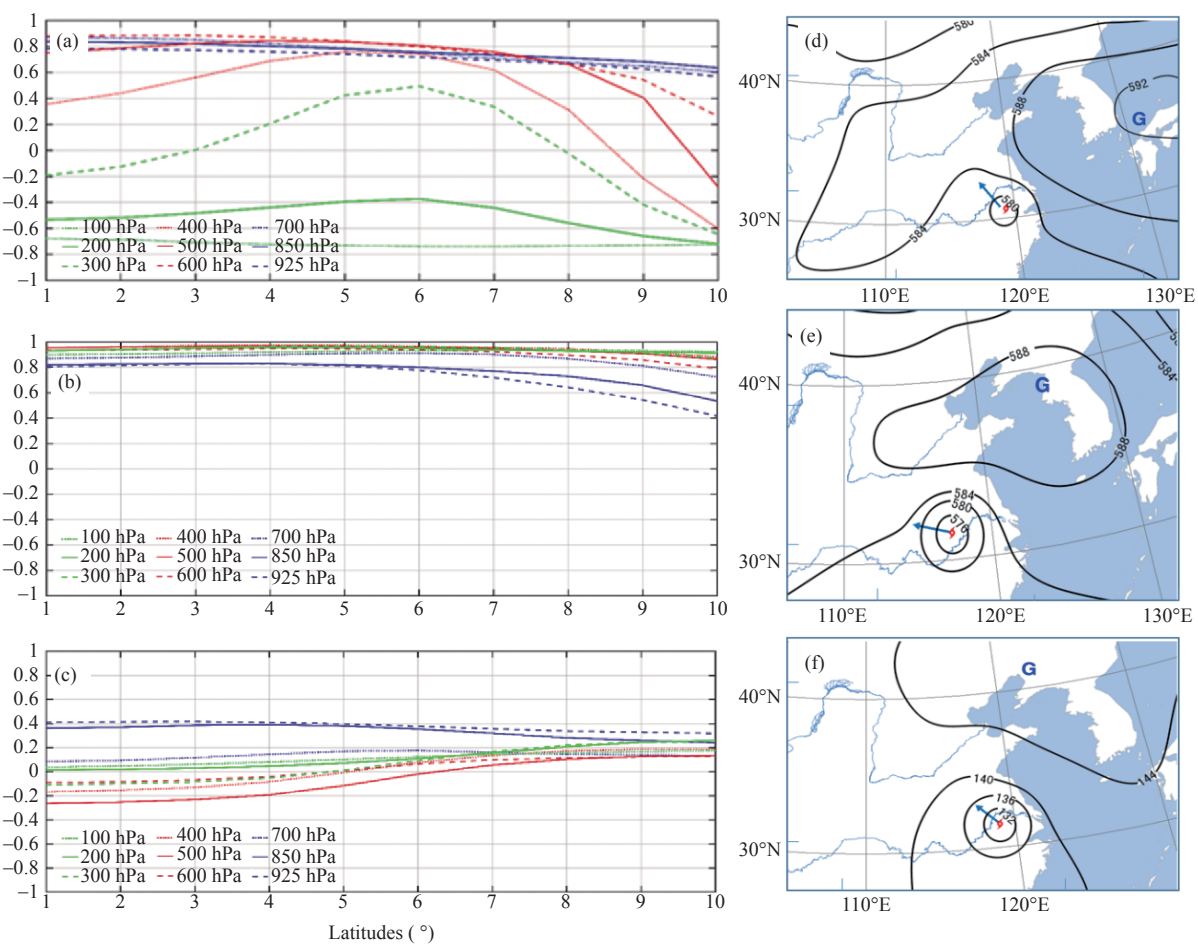

Figure 3. The correlations of the moving speed of (a) Typhoons Yagi (2018), (b) Rumbia (2018), and (c) In-Fa (2021) with the environmental wind fields at different altitudes and latitude distances from the typhoon centers, the 500 hPa geopotential height fields (dagpm) at (d) 0000 UTC on August 13, 2018, and (e) 1200 UTC on August 17, 2018, and (f) the 850 hPa geopotential height field (dagpm) at 0000 UTC on July 27, 2021.

environmental wind fields at different levels and latitude distances from the typhoon centers. The results indicate that the speed of Typhoon Yagi (2018) has the best correlation with 500 hPa and 600 hPa wind fields at 5 latitudes from the typhoon center, with correlation coefficients of up to 0.84 (Fig. 3a). The speed of Typhoon Rumbia (2018) best correlates with the 500 hPa wind field at 5 latitudes from the typhoon center, with a correlation coefficient of 0.97 (Fig. 3b). Unlike the above two typhoons, the speed of Typhoon In-Fa (2021) has the best correlation with the 925 hPa and 850 hPa wind fields at 5 latitudes from the typhoon center, with correlation coefficients of around 0.41 (Fig. 3c).

According to the correlation between the speed of the three typhoons and their corresponding environment wind fields, we can determine the difference in the steering flow of the three typhoons. Fig. 3d shows the 500 hPa geopotential height field of Typhoon Yagi at 0000 UTC on August 13, 2018. Typhoon Yagi was located on the southwestern side of the western Pacific subtropical high (WPSH), with only one closed contour circle and a small range. The core area of the WPSH was located in southern Japan, which had a broader range and stronger intensity than the typhoon. The typhoon moved northwest along the edge of the WPSH, at which time the 500 hPa steering flow was about 12 m s^{-1}. In terms of the 500 hPa geopotential height field at 1200 UTC on August 17, 2018 (Fig. 3e), Typhoon Rumbia was located on the southern side of the WPSH, with two closed contour circles. Simultaneously, the WPSH shows an east-west distribution and controls the area from North China to the Korean Peninsula. Typhoon Rumbia moved westward under the action of the easterly airflow at the periphery of the WPSH. At this time, the steering flow was about 10 m s^{-1}. For the 850 hPa geopotential height field at 0000 UTC on July 27, 2021 (Fig. 3f), Typhoon In-Fa had two closed circles with a strong intensity. The WPSH was located on the northern side of this typhoon. Although the WPSH also showed a zonal distribution, it had no apparent high-pressure center. At this time, the environmental steering flow was only 2 m s^{-1}. From the above analysis, it can be seen that the steering flow of Typhoon In-Fa is much smaller than those of the two typhoons, which may be one reason for its slow movement. As for why the correlation of Typhoon In-Fa is so much less than the correlations of the other two typhoons, and the best correlation level appears in the lower troposphere, this needs further study.

4.2 *Effect of the diabatic heating*

Based on the atmospheric horizontal motion equation, continuity equation, and thermodynamic equation, He developed the motion equation of the air particle in the typhoon center, as shown in Eq. 4 [41]. It approximates the typhoon system as a cylinder bordered by $Z = Z_b$ (lower boundary) and $Z = Z_p$ (upper boundary), with the horizontal area of σ and the volume of τ. In the motion equation, the acceleration ($\mathrm{d}v/\mathrm{d}t$) of typhoon caused by diabatic heating can be approximately expressed as:

$$\frac{\mathrm{d}v}{\mathrm{d}t} = \frac{1}{MC_p\langle T\rangle}\int_\tau Q\overline{V}\rho \mathrm{d}\tau \approx \frac{1}{C_p\langle T\rangle}\overline{(Q\overline{V})} \tag{4}$$

where M is the air mass in the volumn τ, C_p is the specific heat capacity at constant volume, $\langle\rangle$ represents the volume average in the system, $\overline{(\ )}$ represents the horizontal area average, ρ is air density, T is temperature, $\vec{V}$ is the horizontal velocity of the air particle, and Q is the non-adiabatic heating rate. $Q\vec{V}$ represents the product of the diabatic heating rate and the local steering flow velocity, called the diabatic steering flow velocity. The magnitude of $Q\vec{V}$ is proportional to Q and $\vec{V}$, and its direction depends on Q. When $Q > 0$ (heating), the direction of $Q\vec{V}$ coincides with $\vec{V}$, while $Q < 0$ (cooling) indicates the direction of $Q\vec{V}$ is opposite to $\vec{V}$. Based on Eq. 4, it can be found that the effect of the diabatic heating relies on the asymmetry of $Q\vec{V}$. That is, if $Q\vec{V}$ is axis-symmetric in the X-Y coordinate system with the typhoon center as the origin, the right side of Eq. 4 is equal to 0. In this case, no matter how strong the heating is, the movement of the typhoon can not be changed (He [41]).

Figure 4 shows the spatial distributions of the diabatic heating (sum of sensible and latent heat fluxes) and wavenumber-1 asymmetry of the diabatic heating within 5 latitudes from the three typhoon centers during the comparative periods. Obviously, all three typhoons have northwestward tracks. As can be seen from Fig. 4 (a-c), the diabatic heating within 5 latitudes from the three typhoon centers is all positive, indicating that the land heats the atmosphere, but the distributions of the diabatic heating are not uniform. In order to clearly identify the asymmetry of the diabatic heating, the spatial distributions of wavenumber-1 asymmetry of the diabatic heating of the three typhoons are drawn by using the method of Fourier expansion along the orientation (Reasor et al. [42]; Marks et al. [43]). A pair of positive and negative centers with an absolute value of about 80 w m^{-2} are located in the right rear and left front of the centers of Typhoon Yagi (2018) (Fig. 4d). The absolute value of a pair of positive and negative centers in Typhoon Rumbia (2018) can reach 100 w m^{-2} (Fig. 4e). Although Typhoon In-Fa (2021) also have the asymmetry of wavenumber-1 diabatic heating, its positive center with only 40 w m^{-2} is located at the right side 4−5 latitudes from the typhoon center, while its negative center with the absolute value of about 60 w m^{-2} on the left is 2 latitudes from the typhoon center. At a 4−5 latitude distance to the left, the wavenumber-1 diabatic heating flux turns positive again, and the value is larger (Fig. 4f). This configuration makes the asymmetry decrease significantly. In Eq. 4, C_p is a constant, about 1.2 KJ m^{-3} $°C^{-1}$, if the temperature and wind speed of 500 hPa of the three typhoons during the comparison periods are substituted into the formula, the acceleration of typhoons Yagi, Rumbia, and In-Fa can be approximately equal to 1.6 m s^{-2}, 0.9 m s^{-2}, and 0.024 m s^{-2},respectively. It

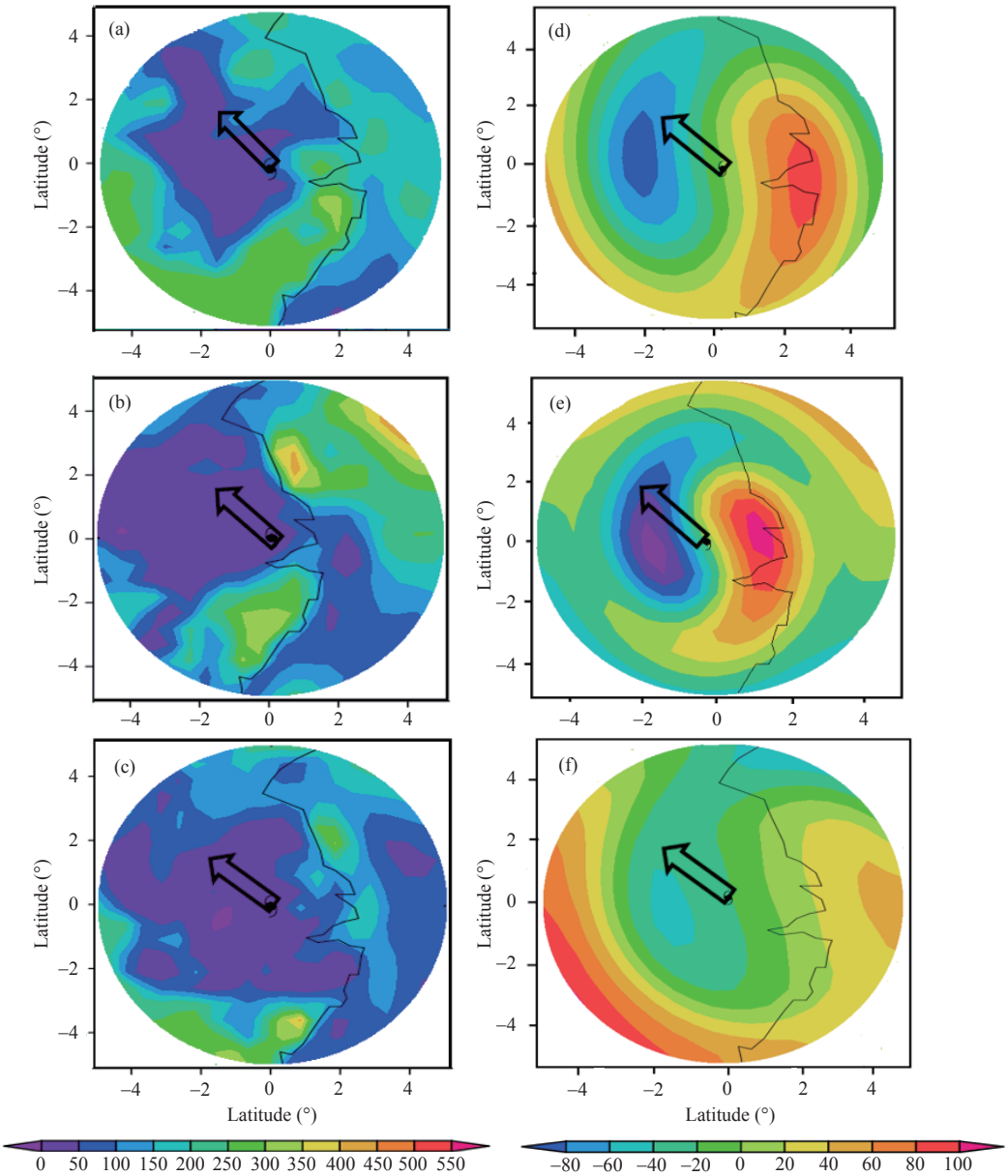

Figure 4. Spatial distributions of the diabatic heating fluxes (a, b, c) and wavenumber-1 asymmetric of the diabatic heating (d, e, f) of the three typhoons within 5 latitudes from the typhoon centers during the comparative periods. (a, b) Typhoon Yagi, (c, d) Typhoon Rumbia and (e, f) Typhoon In-Fa. The arrow represents the direction of the typhoon's movement, and the solid black line shows the coastline.

can be seen that the Typhoon In-Fa movement caused by the asymmetry of the diabatic heating is lower than that of the other two typhoons.

4.3 *Effect of the VWS*

Many tropical cyclones (TCs) occur in the earth's environment with VWS. As the VWS is imposed on a TC, the TC vortex tends to tilt, resulting in asymmetries in the convection as well as the dynamic and thermodynamic fields, which change the structure of the typhoon (Frank and Ritchie [44]). As shown in Fig. 5, the evolution of the VWS of the three typhoons indicates that the wind shear of the three typhoons is quite weak in the first hour, with an intensity of less than 5 m s^{-1}. After 2 hours, the wind shear of Typhoons Yagi (2018) and Rumbia (2018) began to strengthen, while the wind shear of Typhoon In-Fa (2021) began to weaken. In the whole comparison stage, the wind shear values of the first two Typhoons are mostly at moderate intensity (5−10 m s^{-1}), while the latter is at weak intensity (<5 m s^{-1}).

The structural changes of three typhoons are compared by selecting the periods with large differences in VWS. As seen from Fig. 6, the vertical wind shear values of Typhoons Yagi and Rumbia are relatively large, which are 9.6 m s^{-1} and 10.3 m s^{-1}, respectively, and the directions are both northward. The vertical wind shear value of Typhoon In-Fa is only 1.8 m s^{-1}, and the direction is to the east. Combined with radar echoes, the first two typhoon structures showed obvious asymmetry, and the

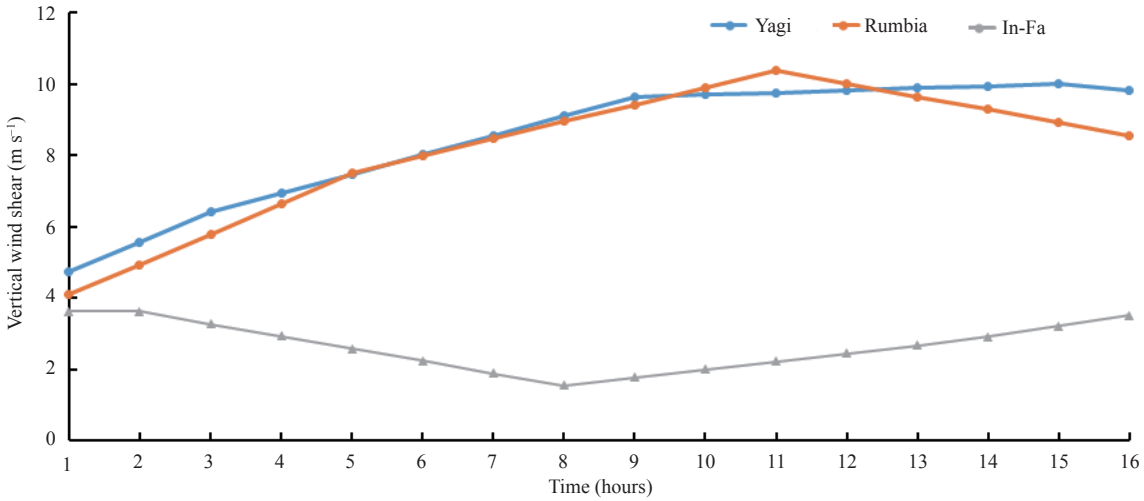

Figure 5. Evolution of the VWS of Typhoons Yagi (2018), Rumbia (2018) and In-Fa (2021). The *X*-axis presents the comparative periods, where "1" indicates the first hour of the comparative periods.

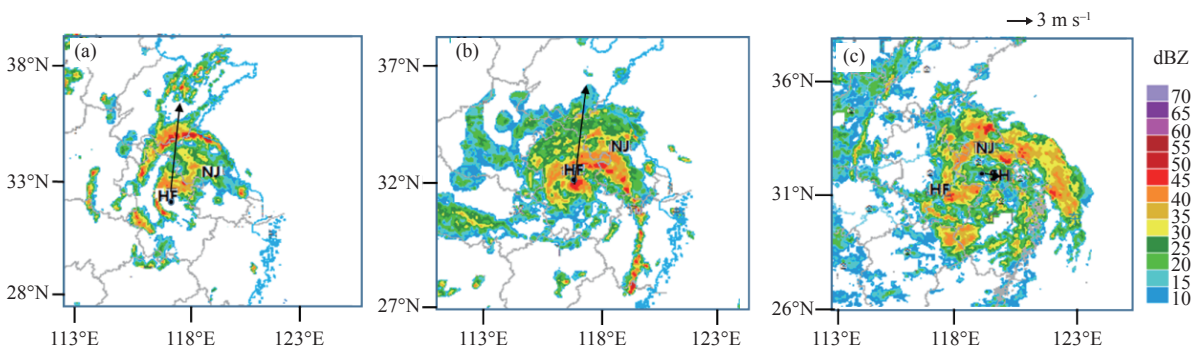

Figure 6. Radar composite reflectivity images of (a) Typhoon Yagi at 0600 UTC on August 13, 2018, (b) Typhoon Rumbia at 1200 UTC on August 17, 2018, and (c) Typhoon In-Fa at 0000 UTC on July 27, 2021. Arrows indicate the direction and magnitude of VWS, the black dot indicates the center of the typhoon, and the acronyms stand for stations Hefei (HF), Nanjing (NJ), and Shanghai (SH).

cloud bands were mainly concentrated on the north and west sides of the typhoon, which was related to the high vertical wind shear value (Wang et al. [45]). The asymmetric structure of the typhoon weakens its strength and leads to the reduction of internal force. The latter typhoon is basically circular in structure, and the lowest surface pressure in the center of the typhoon is 982 hPa, which is lower than the previous two typhoons (985 hPa and 982 hPa, respectively), indicating that its internal force is also greater than the previous two typhoons. The greater the internal force of a typhoon, the stronger the typhoon, and the slower the typhoon′s moving speed. It can be seen that vertical wind shear changes the typhoon's structure, makes the typhoon's strength change, and ultimately affects the typhoon′s moving speed.

4.4 *Effect of the surface synoptic situation*

Generally, surface cyclones move along the direction of the allobaric gradient, and their moving speed is proportional to the allobaric gradient and inversely proportional to the intensity of the vortex center (Zhu et al. [36]). In the surface situation map at 0000 UTC on August 13, 2018 (Fig. 7a), Typhoon Yagi (2018) is located at 30.7°N, 119.3°E, with a central pressure of 995 hPa and maximum wind speed of 18 m s^{-1} at the typhoon center near the surface. The typhoon structure is asymmetric, with dense isobars on the north side and sparse ones on the south side. The main precipitation areas are concentrated near typhoon center and on the northern side of the typhoon. An apparent negative pressure change zone is formed in the typhoon center and its northern side within 350 km. The negative pressure change center is close to the typhoon center, with a value of −28 hPa. Thus, Typhoon Yagi moved along the direction of the allobaric gradient.

The surface situation map at 1200 UTC on August 17, 2018 (Fig. 7b) indicates that Typhoon Rumbia (2018) is centered at 31.1°N, 120.6°E, with a central pressure of 985 hPa and maximum wind speed of 23 m s^{-1} at the typhoon center, which has stronger intensity than Typhoon Yagi. The isobars at the typhoon center are nearly circular, and the peripheral isobars on the northern side are denser than those on the southern side. Precipitation mainly occurs on the northwestern side of the typhoon. The negative pressure change zone of the typhoon extends westward from the typhoon center. The pressure change center is close to the typhoon center, with a value of −39

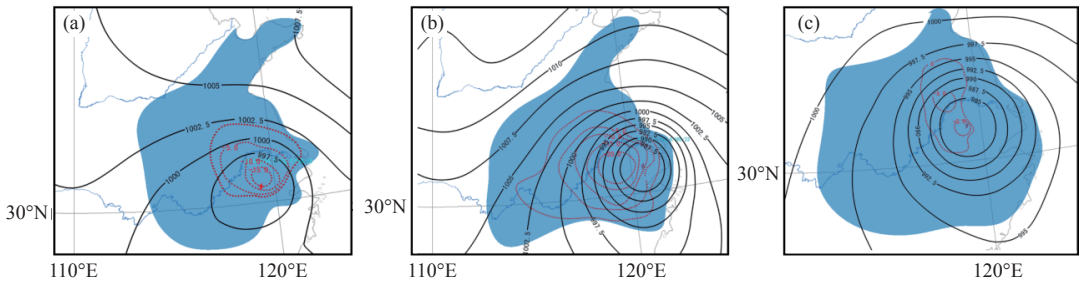

Figure 7. The surface situation maps of (a) Typhoon Yagi at 0000 UTC on August 13, 2018, (b) Typhoon Rumbia at 1200 UTC on August 17, 2018, and (c) Typhoon InFa on July 27, 2021. The solid lines represent the isobaric lines (hPa), the dashed lines indicate the 3-hour pressure change (hPa), and the shaded areas denote the 6-hour precipitation (mm).

hPa. Thus, Typhoon Rumbia also moved along the direction of the allobaric gradient.

In the surface situation map of Typhoon In-Fa (2021) at 0000 UTC on July 27, 2021 (Fig. 7c), the typhoon is located at 31.3°N, 119.4°E, with a central pressure of 982 hPa and a maximum wind speed of 20 m s^{-1} at the typhoon center. The isobars surrounding the typhoon are dense and nearly circular. The heavy precipitation is concentrated on the dense isobars at the typhoon center. The negative pressure change areas in the typhoon center and its northern side are small, with a weak intensity of only about −7 hPa, surrounded by a larger area of strong and positive pressure change.

Overall, the central pressure of Typhoon In-Fa is the strongest among the three typhoons. Additionally, there is no apparent allobaric gradient in front of Typhoon In-Fa. According to the mechanisms of cyclone movement, i.e., the speed of cyclones is proportional to allobaric gradient and inversely proportional to their intensity, Typhoon In-Fa moved slower than Typhoons Yagi and Rumbia.

4.5 *Physical mechanism of low moving speed of landing Typhoon In-Fa*

After Typhoon In-Fa (2021) landed in Zhejiang Province, its moving speed has been around 10 km h^{-1} for several days. Through the analysis results in the above sections, several key factors that affect the moving speed of typhoons can be summarized. Without considering the change of underlying surface, the moving speed of a landing typhoon mainly depends on two aspects: one is the large-scale environmental background field. The movement of typhoons largely depends on the steering flow. Under the same conditions, typhoons with strong steering flow move faster. In addition, the VWS of the environment can also indirectly affect the movement of typhoons. As the VWS is imposed on a typhoon, the typhoon tends to tilt, resulting in asymmetries in the convection. Convective clouds often occur in the direction of the shear and its left side to change the structure of the typhoon, weaken the strength of the typhoon, and ultimately affect the moving speed of the typhoon (Wang et al. [27]). The second is the typhoon itself. According to Zhu et al. [36], the stronger the cyclone, the slower its speed, and the cyclone moves in the direction of the pressure gradient. During the comparison period, the intensity of Typhoon In-Fa is slightly stronger than that of Typhoon Yagi and Rumbia, and the pressure gradient in front of Typhoon In-Fa is obviously smaller than that of the latter, which results in the slow movement of Typhoon In-Fa. In addition, the precipitation of Typhoon In-Fa is around its center, while the precipitation of Typhoons Yagi and Rumbia is mainly concentrated on the west and north sides of typhoons, showing obvious asymmetry of precipitation distribution. A large amount of latent heat of condensation is released in the distribution area of heavy precipitation. As a result, Typhoons Yagi and Rumbia have a significant asymmetry of wavenumber-1 diabatic heating compared to Typhoon In-Fa. The diabatic heating causes the air in front of the moving direction of the typhoon to heat up, the corresponding gas column to lengthen, and the surface pressure to drop, thus increasing the pressure gradient near the center of the typhoon. This is also one reason why Typhoons Yagi and Rumbia move faster than Typhoon In-Fa.

5 CONCLUSIONS AND DISCUSSION

After Typhoon In-Fa (2021) made landfall, its moving speed remained at or below 10 km h^{-1}, noticeably slower than that of other landfalling typhoons. To explore the causes of the low moving speed, Typhoons Yagi (2018) and Rumbia (2018), which are similar to Typhoon In-Fa (2021) in the tracks, intensity, and underlying surface conditions, are selected in this research to perform a comparative analysis based on steering flow, diabatic heating, VWS, and surface synoptic situation. The main conclusions are as follows.

The moving speed of Typhoons Yagi and Rumbia best correlates with their corresponding 500 hPa environmental wind fields, with the speed of steering flow being 10–12 m s^{-1}. The moving speed of Typhoon In-Fa has the best correlation with the 850 hPa and 925 hPa environmental wind fields, and its steering flow has a speed of only 2 m s^{-1}. The weak steering flow is one of the reasons for the low moving speed of Typhoon In-Fa.

In the areas within 5 latitudes from three typhoon centers, the diabatic heating fluxes of the three typhoons are all positive, and there are wavenumber-1 asymmetric structure distributions. Among them, Yagi and Rumbia have high asymmetry, and the positive and negative

centers are located on the left and right sides of the typhoons' moving direction, with an absolute value above 80 w m^{-2}. However, the positive center of Typhoon In-Fa is located on the right side, about 5 latitude distance from the typhoon center, while the negative center is on the left side, about 2 latitude distance from the typhoon center. The positive and negative centers are asymmetric to the typhoon center. According to formula 4, the acceleration of typhoons Yagi, Rumbia, and In-Fa can be approximately equal to 1.6 m s^{-2}, 0.9 m s^{-2}, and 0.024 m s^{-2}, respectively.

Compared with Typhoons Yagi and Rumbia, Typhoon In-Fa has the lowest central pressure and the densest isobar distribution. The allobaric gradient in the northwest direction of Typhoon Yagi and Rumbia is obviously larger than that of Typhoon In-Fa. The configuration of this ground situation has also become a reason for the low moving speed of Typhoon In-Fa.

In this study, we discuss the causes of the low moving speed of Typhoon In-Fa (2021) based on steering flow, diabatic heating, VWS, and surface synoptic situation. However, there are many other factors affecting typhoon moving speed, such as temperature, temperature advection, the vorticity in the typhoon environmental field, the internal force and structure of typhoons, topographic forcing, and frictional effects might affect typhoon moving speed. All these factors cannot be covered in this research. The moving speed of typhoons can impact the choice of timing for defense, which is crucial for disaster prevention and mitigation. In the future, we will continue to research the moving speed of typhoons based on the influencing factors and strive to improve the forecast of typhoon tracks.

REFERENCES

[1] CHEN S J, KUO Y H, ZHANG P Z, et al. Climatology of explosive cyclones off the East Asian Coast [J]. Monthly Weather Review, 1992, 120(12): 3029–3035, https://doi.org/10.1175/1520-0493(1992)1202.0.CO;2

[2] ZHANG J Z, XU H M, MA J, et al. Interannual variability of spring extratropical cyclones over the Yellow, Bohai, and East China Seas and possible causes [J]. Atmosphere, 2019, 10(1): 40, https://doi.org/10.3390/atmos10010040

[3] FU G, SUN Y W, SUN J L, et al. A 38-year climatology of explosive cyclones over the Northern Hemisphere [J]. Advances in Atmospheric Sciences, 2020, 37(2): 143–159, https://doi.org/10.1007/s00376-019-9106-x

[4] CHAN J C, WILLIAMS R T. Analytical and numerical studies of the beta-effect in tropical cyclone motion, Part I: Zero mean flow [J]. Journal of Atmospheric Science, 1987, 44: 1257–1264.

[5] WANG B, ELSBERRY R L, WANG Y Q, et al. Dynamics in tropical cyclone motion: a review [J]. Journal of Atmospheric Science, 1998, 22(4): 535–547.

[6] CHEN S S, KNAFF J A, MARKS F D. Effects of vertical wind shear and storm motion on tropical cyclone rainfall asymmetries deduced from TRMM [J]. Monthly Weather Review, 2006, 134(11): 3190–3208.

[7] ZHU L J, LIN F L, LIANG C J. Modulation of tropical cyclone activity over the northwestern Pacific through the quasi-biweekly oscillation [J]. Journal of Tropical Meteorology, 2021, 27(2): 125–134.

[8] YUAN Jun-peng, CAO Jie. North Indian Ocean tropical cyclone activities influenced by the Indian Ocean Dipole mode [J]. Science in China, Series D: Earth Sciences, 2013, 56(5): 855–865.

[9] FAN Xiao-ting, LI Ying, LÜ Ai-min, et al. Statistical and comparative analysis of tropical cyclone activity over the Arabian Sea and Bay of Bengal (1977–2018) [J]. Journal of Tropical Meteorology, 2020, 26(3): 441–452, https://doi.org/10.46267/j.1006-8775.2020.038

[10] BENDER M A, TULERA R E, KURIHARA Y. A numerical study of the effect of island terrain on tropical cyclones [J]. Monthly Weather Review, 1987, 115: 130–155.

[11] CHEN L S, YING L, CHENG Z Q. An overview of research and forecasting on rainfall associated with land-falling tropical cyclones[J]. Advances in Atmospheric Sciences, 2010, 27(5): 967–976.

[12] HAN Fu-rong, LU Xiang, FENG Xiao-yu, et al. Analysis of dynamic and thermodynamicg structure of Typhoon lekima (1909) before and after its landfall [J]. Journal of Tropical Meteorology, 2021, 37(1): 34–48, in Chinese with English abstract.

[13] HUANG L, WEN Y F, LIU Y D. Formation and replacement mechanism of the concentric eyewall of super typhoon Muifa (1109) [J]. Journal of Tropical Meteorology, 2022, 28(4): 425-444, https://doi.org/10.46267/j.1006-8775.2022.032.

[14] WU C C, YEN T H, KUO Y H, et al. Rainfall simulation associated with typhoon Herb (1996) near Taiwan, Part I: The topographic effect [J]. Weather Forecasting, 2002, 17 (5): 1001–1015.

[15] LI Ze-chun, CHEN Yun, ZHANG Fang-hua, et al. Reflections caused by the "75.8" heavy rain in Henan [J]. Meteorological and Environmental Sciences, 2015, 38(3): 1–12, in Chinese with English abstract

[16] ZHENG Li-na, WANG Yuan, ZHANG Zi-han. Causal analysis of extra torrential rain of typhoon Lekima in Shandong in 2019 [J]. Meteorological Science and Technology, 2021, 49: 437–445, in Chinese with English abstract

[17] YANG Y T, KUO H C, HENDRICKS E A, et al. Structural and intensity changes of concentric eyewall typhoons in the western North Pacific basin [J]. Monthly Weather Review, 2013, 141(8): 2632–2648, https://doi.org/10.1175/MWR-D-12-00251.1

[18] HILL K A, LACKMANN G M. Influence of environmental humidity on tropical cyclone size [J]. Monthly Weather Review, 2009, 137(10): 3294–3315, https://doi.org/10.1175/2009 MWR2679.1

[19] ZHANG Zhong-feng, LIU Qi-han. Numerical study of typhoon Maggie's track anomaly [J]. Journal of Tropical Meteorology, 2006, 22: 55–59, in Chinese with English abstract

[20] MA Jing-xian, MA Fen-hua, WANG Yong-qing. Dipole flow effects on typhoon 9408 track [J]. Journal of Nanjing Institute of Meteorology, 2001, 24: 338–342, in Chinese with English abstract

[21] DUAN Jing-jing, WU Li-guang, NI Zhong-ping. Analysis of unusual changes in Typhon Aere (2004) and Meari (2004) [J]. Acta Meteorologica Sinica, 2014, 72: 1–11, in

Chinese with English abstract
[22] ZHENG Li-na, XIA Jin-ding, WANG Jun-xi. Analysis of previous signals of two land-falling typhoons during those movement northward in August 2018 [J]. Journal of Catastrophology, 2019, 34: 131–136, in Chinese with English abstract
[23] ZHANG Z H, ZHENG L N. Forecasting factors of the northward sharp turn of typhoons that make landfall [J]. Marine Forecasts, 2020, 37: 46–53, in Chinese with English abstract
[24] WANG T, PENG Y H, ZHANG B L, et al. Move a tropical cyclone with 4D-VAR and vortex dynamical initialization in WRF model [J]. Journal of Tropical Meteorology, 2021, 27(3): 191–200.
[25] YUAN Jin-nan, GU De-jun, LIANG Jian-yin. A study of the influence of topography and boundary layer friction on landfalling tropical cyclone track and intensity [J]. Chinese Journal of Atmospheric Sciences, 2005, 29(3): 429–437, in Chinese with English abstract
[26] LI X, PU Z. Sensitivity of numerical simulation of early rapid intensification of Hurricane Emily (2005) to cloud microphysical and planetary boundary layer parameterizations [J]. Monthly Weather Review, 2008, 136(12): 4819–4838, https://doi.org/10.1175/2008MWR2366.1
[27] WANG C X, YING M. The uncertainty of tropical cyclone intensity and structure based on different parameterization schemes of planetary boundary layer [J]. Journal of Tropical Meteorology, 2020, 26(4): 377–389.
[28] HUANG R H, CHEN G H. Research on interannual variations of tracks of tropical cyclones over northwest Pacific and their physical mechanism [J]. Acta Meteorologica Sinica, 2007, 65: 683–694, in Chinese with English abstract
[29] ZHANG S M, WANG K, SUN G, et al. Analysis of the causes of local heavy rain caused by residual low pressure of Typhoon Nepartak [J]. Meteorological Science and Technology, 2018, 46: 139–147, in Chinese with English abstract
[30] ZHAO H K, JIANG X N, WU L G. Modulation of northwest Pacific tropical cyclone genesis by the intraseasonal variability [J]. Journal of the Meteorological Society of Japan, 2015, 93: 81–97.
[31] POWELL M D, VICKERY P J, REINHOLD T A. Reduced drag coefficient for high speeds in tropical cyclones [J]. Nature, 2003, 422(3): 279–283, https://doi.org/10.1038/nature01481
[32] ZHAO Z. Multi-satellite observations on the structure characteristics of typhoon Meranti in 2016 [J]. Plateau Meteorology, 2019, 38(1): 156–164, in Chinese with English abstract
[33] ZENG Zhi-hua, CHEN Lian-shou, WANG Yu-qing, et al. A numerical simulation study of super Typhoon Saomei (2006) intensity and structure changes [J]. Acta Meteor Sinica, 2009, 67(5): 750–763, https://doi.org/10.1016/S1874-8651(10)60080-4, in Chinese with English abstract
[34] SMITH R K, THOMSEN G L. Dependence of tropical cyclone intensification on the boundary layer representation in a numerical model [J]. Quarterly Journal of the Royal Meteorological Society, 2010, 136(10A): 1671–1685, https://doi.org/10.1002/qj.687
[35] YANG L, DU Y, WANG D X, et al. Impact of intraseasonal oscillation on the tropical cyclone track in the South China Sea [J]. Climate Dynamics, 2015, 44: 1505–1519.
[36] ZHU Q G, LIN J R, SHOU S W, et al. Principles and Methods of Synoptic Meteorology [M]. Beijing: Meteorological Press, 1992: 203–215, in Chinese
[37] WU L, WANG B. A potential vorticity tendency diagnostic approach for tropical cyclone motion [J]. Monthly Weather Review, 2000, 128: 1899–1911.
[38] WINGO M T, CECIL D J. Effects of VWS on tropical cyclone precipitation [J]. Monthly Weather Review, 2010, 138: 645–662.
[39] ADEM J, LEZAMA P. On the motion of a cyclone embedded in a uniform flow [J]. Tellus, 1960, 12: 255–258.
[40] CHAN J C, GRAY W M. Tropical cyclone movement and surrounding flow relationships [J]. Monthly Weather Review, 1982, 110: 1354–1374.
[41] HE H Y. A study on typhoon movement I: The effect of diabatic heating and horizontal temperature distribution [J]. Journal of Tropical Meteorology, 1995, 11: 1–9, in Chinese with English abstract
[42] REASOR P D, MONTGOMERY MT, MARKS F D, et al. Low-wavenumber structure and evolution of the hurricane inner core observed by airborne dual-doppler radar [J]. Monthly Weather Review, 2000, 128: 1653–1680.
[43] MARKS F D, HOUZE R A, GAMACHE J F. Dual-aircraft investigation of the inner core of Hurricane Norbert, Part Ⅰ: Kinematic structure [J]. Journal of Atmospheric Sciences, 1992, 49: 919–942.
[44] FRANK W M, RITCHIE E A. Effects of vertical wind shear on the intensity and structure of numerically simulated hurricanes [J]. Monthly Weather Review, 2001, 129(9): 2249–2269.
[45] WANF C D, FANG J, MA Y M. Structural changes preceding the rapid intensification of Typhoon Lekima (2019) under moderate vertical wind shear [J]. Journal of Geophysical Research: Atmospheres, 2022, 127: e2022JD036544, https://doi.org/10.1029/2022JD036544

Citation: ZHENG Li-na, LÜ Xin-gang, LI Rui. An Analysis of the Low Moving Speed of Landfalling Typhoon In-Fa in 2021 [J]. Journal of Tropical Meteorology, 2024, 30(1): 51-60, https://doi.org/10.3724/j.1006-8775.2024.006